Real-Time Position Determination on the Mars Surface Using Relative Joint Doppler and Ranging Measurements

William Jun,* Kar-Ming Cheung,† E. Glenn Lightsey,‡ Charles Lee†

ABSTRACT. — A positioning and timing (PNT) solution is essential for conducting operations on the surface of a planetary body. The Joint Doppler and Ranging (JDR) scheme was introduced in prior papers to provide real-time 3D position determination for a user on the lunar surface. This paper proposes and analyzes an in-situ relay architecture that uses relative JDR to obtain real-time position estimates of a user on the surface of Mars. JDR with the Law of Cosines (LOC) utilizes a novel Doppler based approach in addition to range measurements for relative navigation. Although the LOC method requires a reference station, it facilitates the use of Doppler-derived pseudorange equations, which allow for positioning with only Doppler measurements. This Doppler-only method is then modified to include range measurements, which enable precise real-time positioning with only a few navigational nodes (as few as a single orbiter). In this analysis, the user and a reference station were simulated on the surface of Mars with a maximum of two orbiters in view. Orbiter ephemeris, velocity, and measurement errors were modeled as Gaussian variables in a Monte Carlo analysis. The simulated measurements were processed by a JDR-based Kalman Filter to calculate a real-time estimate of the user's position. The resulting 3D root mean squared error for position estimates ranged from under 40 meters for the nominal error cases to under 5 meters for the optimistic error cases. Ultimately, this analysis describes a viable implementation of an in situ relay PNT solution on the surface of Mars. JDR enables real-time PNT knowledge for surface users with a minimal required infrastructure.

I. Introduction

Exploration on the Mars surface requires precise knowledge of position and timing. However, the round-trip time for communications between Mars and Earth can be up to 40 minutes, leading to the necessity of autonomous navigation for complex exploration missions. Real-time positioning would further enable this autonomy. Therefore, there is a

* Communications Architectures and Research Section; and also, Georgia Institute of Technology.

† Communications Architectures and Research Section.

‡ Georgia Institute of Technology.

The research described in this publication was carried out with the Jet Propulsion Laboratory, California Institute of Technology, under a contract with the National Aeronautics and Space Administration.

growing need for a navigation architecture on Mars that can be autonomous and sustainable for the future.

Currently, navigation of Martian rovers is performed through terrain mapping and modelling [1, 2, 3]. This approach requires extensive terrain measurements, and significant data fusion to construct high-fidelity surface topographic maps. One of many proposed solutions for autonomous navigation includes mimicking a carrier-phase differential Global Positioning System (GPS) on Mars through an array of transmitters distributed on the surface [4]. This may achieve sub-meter level positioning accuracy, but also requires a large navigation infrastructure to be built before utilization. This paper proposes the use of relative Joint Doppler and Ranging (JDR) to provide real time, 3D position determination on the Martian surface with a minimal navigational infrastructure.

JDR utilizes both range and Doppler measurements in a novel approach to position a user [5]. JDR consists of two methods, the Law of Cosines (LOC) scheme and Conic Doppler Localization (CDL). LOC is a relative navigation architecture that converts Doppler measurements into Doppler-derived range with the aid of a reference station and at least one orbiter [6]. Previously, these JDR methods were simulated on the Moon through Doppler Based Autonomous Navigation (DBAN) to position a user in orbit [7]. The DBAN analysis considered dynamic users in orbit, while this paper analyzed a static user on the surface of the planet.

In this paper, JDR-LOC was used to localize a static user with a known reference station located on the equator of Mars. Three equatorial orbiters with an inclined orbiter were used with the reference station located 15 km from the user. Two way ranging and Doppler measurements were made from each visible orbiter every minute during the analysis interval of approximately 8 hours.

An extended Kalman filter (EKF) with JDR-LOC was implemented and a Monte Carlo analysis was performed with 1000 iterations. These analyses included embedded error on both range and Doppler measurements and orbiter ephemeris knowledge. Additionally, the user was limited with a 15-degree elevation mask.

Ultimately, JDR-LOC provided accurate, real-time position knowledge to a surface user on Mars with a minimal navigation infrastructure. Although this analysis was only for a single scenario, JDR can be used with any other navigation infrastructure with a minimum of one orbiter. This enables autonomous positioning not only for Mars, but any planetary body with an orbiter and with or without a reference station.

II. Review of Joint Doppler and Ranging

JDR consists of two methods: the LOC and CDL. Both methods are utilized in scenarios with a dynamic user, where the line-of-sight to the reference station can be lost. However, the user was assumed to be static and within range of the reference station in this analysis. Therefore, only the relative method, LOC, was used.

A. Joint Doppler and Ranging – Law of Cosines

The LOC scheme is a relative Doppler based positioning scheme that requires a reference station and as few as one orbiter to localize a user [5]. A novel process is used in this scheme to convert Doppler measurements into Doppler-based range measurements. These Doppler-based range measurements eliminate shared errors in both the Doppler measurements and orbiter ephemeris knowledge. With the addition of range measurements, the Doppler-derived range can be made more accurate. Since current proximity link radios can log Doppler shifts of locked orbiters in real time, positioning is enabled with relatively low hardware requirements with JDR-LOC.

B. Derivation of JDR-LOC

The Doppler-derived range equation for JDR-LOC can be derived assuming a nearby reference station that can communicate measurements to the user [7]. Figure 1 describes the geometry between the user, satellite, and reference station.

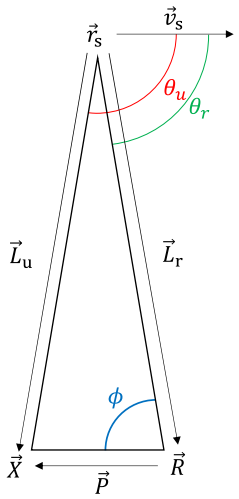

Figure 1. LOC geometry.

Where $\vec{X}$ is the user, $\vec{R}$ is the reference station, $\overrightarrow{r_s}$ is the current satellite, $\overrightarrow{v_s}$ is the current satellite's velocity vector, and $\vec{P}$ is the relative positioning vector from the reference station to the user. In addition, $\overrightarrow{L_u}$ and $\overrightarrow{L_r}$ are the line of sight vectors from the satellite to the user and reference station, respectively.

Then, the Doppler shifted frequency received by the user is defined as:

$$f_u = \left(\frac{c+\dot{r}_u}{c}\right) f_0 \,, \tag{1}$$

where f_0 is the transmitted frequency, f_u is the user's received frequency, $\dot{r}_u$ is the line of sight range rate, and c is the speed of light. Assuming $\Delta f_u = f_u - f_0$, Equation (1) is rearranged to solve for $\dot{r}_u$ as a function of the user's Doppler measurement Δf_u.

$$\dot{r}_u = \left(\frac{\Delta f_u}{f_0}\right) c \tag{2}$$

Knowing that the range rate is the projection of the satellite's velocity vector $\overrightarrow{v_s}$ onto the line of sight vector $\overrightarrow{L_u}$, the angle between the two vectors can be calculated:

$$\cos\theta_u = \frac{\Delta f_u c}{f_0 \|\overrightarrow{v_s}\|}. \tag{3}$$

This relationship can be repeated with respect to the reference station.

$$\cos\theta_r = \frac{\Delta f_r c}{f_0 \|\overrightarrow{v_s}\|} \tag{4}$$

Using the definition of the angle between two vectors, the angles θ_u and θ_r can be defined:

$$\cos\theta_u = \frac{\overrightarrow{L_u}\cdot\overrightarrow{v_s}}{\|\overrightarrow{L_u}\|\|\overrightarrow{v_s}\|}, \quad \cos\theta_r = \frac{\overrightarrow{L_r}\cdot\overrightarrow{v_s}}{\|\overrightarrow{L_r}\|\|\overrightarrow{v_s}\|}. \tag{5}$$

These can be rearranged to solve for the range values $\|\overrightarrow{L_u}\|$ and $\|\overrightarrow{L_r}\|$. Substituting the angles with the relations (3) and (4):

$$\|\overrightarrow{L_u}\| = \left(\overrightarrow{L_u}\cdot\overrightarrow{v_s}\right)\frac{f_0}{c\Delta f_u}, \quad \|\overrightarrow{L_r}\| = \left(\overrightarrow{L_r}\cdot\overrightarrow{v_s}\right)\frac{f_0}{c\Delta f_r}. \tag{6}$$

Knowing that $\overrightarrow{L_u} = \overrightarrow{L_r} + \vec{P}$ and additionally solving for the magnitude of the relative position vector $\vec{P}$:

$$\|\overrightarrow{L_u}\| = \left(\left(\overrightarrow{L_r} + \vec{P}\right)\cdot\overrightarrow{v_s}\right)\frac{f_0}{c\Delta f_u}, \tag{7}$$

$$\|\overrightarrow{L_r}\| = \left(\overrightarrow{L_r}\cdot\overrightarrow{v_s}\right)\frac{f_0}{c\Delta f_r}, \tag{8}$$

$$\|\vec{P}\| = \frac{\vec{P}\cdot(-\overrightarrow{L_r})}{\|\overrightarrow{L_r}\|\cos\phi}. \tag{9}$$

The equations defined above are the Doppler-derived range equations [7]. Knowing that these equations solve for the sides of the triangle shown in Figure 1, the Law of Cosines can be used to relate all three.

$$\|\overrightarrow{L_u}\|^2 = \|\overrightarrow{L_r}\|^2 + \|\vec{P}\|^2 - 2\|\overrightarrow{L_u}\|\|\vec{P}\|\cos\phi \tag{10}$$

$$\left(\left(\left(\overrightarrow{L_r} + \vec{P}\right)\cdot\overrightarrow{v_s}\right)\frac{f_0}{c\Delta f_u}\right)^2 = \left(\left(\overrightarrow{L_r}\cdot\overrightarrow{v_s}\right)\frac{f_0}{c\Delta f_r}\right)^2 + \|\vec{P}\|^2 + 2\vec{P}\cdot\overrightarrow{L_r} \tag{11}$$

This provides an expression relating the Doppler measurements from the user and the reference station to the relative position vector $\vec{P}$ of the user. The vector $\vec{P}$ can be calculated from this expression using root finding algorithms if enough measurements are known. In addition, the expression can be converted into a measurement model and used in a filter to continuously estimate the user's position. During implementation, this expression is rearranged to remove Doppler measurements from the denominators, therefore removing divergence during zero measured Doppler shifts.

Additionally, the standard pseudorange equation is utilized (without clock correction).

$$\|\overrightarrow{L_u}\| = \|(\vec{R} + \vec{P}) - \vec{r_s}\| \tag{12}$$

III. Extended Kalman Filter

An EKF was used to continuously estimate the position of the user. Because the estimated state was defined in the planet fixed frame and the user was static throughout the entire analysis, the dynamics model for the user was simplified to an identity matrix. The EKF process was referenced from [8]

$$\vec{X} = \begin{bmatrix} x \\ y \\ z \end{bmatrix}, \tag{13}$$

$$x_k = f_{k-1}(x_{k-1}, u_{k-1}, w_{k-1}),\ w_k \sim N(0, Q_k)\ , \tag{14}$$

$$y_k = h_k(x_k, v_k),\ v_k \sim N(0, R_k)\ , \tag{15}$$

with a covariance and measurement update:

$$P_k^- = F_{k-1} P_k^+ F_{k-1}^T + Q_{k-1},\ F_k = \begin{bmatrix} 1 & 0 & 0 \\ 0 & 1 & 0 \\ 0 & 0 & 1 \end{bmatrix}, \tag{16}$$

$$K_k = P_k^- H_k^T (H_k P_k^- H_k^T + R_k)^{-1}\ , \tag{17}$$

$$\hat{x}_k^+ = \hat{x}_k^- + K_k\big(y_k - h_k(\hat{x}_k^-, 0)\big), \tag{18}$$

$$P_k^+ = (I - K_k H_k) P_k^-\ , \tag{19}$$

where the measurement model $h_k(\hat{x}_k^-, 0)$ included both Doppler and range measurement equations from JDR-LOC:

$$h_k(\hat{x}_k^-, 0) = \begin{bmatrix} \left(\left(\left(\overrightarrow{L_r} + \vec{P}\right) \cdot \overrightarrow{v_s}\right) \frac{f_0}{c \Delta f_u}\right)^2 - \left(\left(\overrightarrow{L_r} \cdot \overrightarrow{v_s}\right) \frac{f_0}{c \Delta f_r}\right)^2 - \|\vec{P}\|^2 + 2\vec{P} \cdot \overrightarrow{L_r} \\ \|(\vec{R} + \vec{P}) - \vec{r_s}\| \end{bmatrix}. \tag{20}$$

IV. Simulation Scenario

A. User and Reference Station

The user was assumed to be located on the equator, with a longitude of 0 degrees. This location was chosen due to its consistent coverage for inclined orbits [9]. In addition, the reference station was 15 km from the user with continuous communications between both the user and orbiters (during orbiter ground passes). JDR has previously been shown to be robust to the distance between the user and the reference station if the assumption of

continuous communication holds [5]. To account for terrain and atmospheric effects, a 15-degree elevation mask was used for both the user and the reference station. However, no other atmospheric effects were analyzed.

B. Orbital Infrastructure

A total of four orbiters were utilized in this analysis. Three orbiters were in an equatorial constellation, with the final in a lower, inclined orbit. The equatorial constellation was chosen from the assumption of a communications/navigation constellation around Mars with global coverage of the Martian equator. The inclined orbiter was assumed to be a pre-existing orbiter that could be included into the navigation infrastructure. Note that the orbital infrastructure used in this analysis is not a requirement; JDR could be utilized with any pre-existing navigation infrastructure.

Table 1. Orbital elements.

Orbiter	h (km)	i (deg)	Ω (deg)	w (deg)
Equatorial 1	3000	0	0	0
Equatorial 2	3000	0	120	0
Equatorial 3	3000	0	240	0
Inclined	450	29	25	337

Figure 2 describes the trajectories of each orbiter during the analysis interval. Also included (in green) are the portions of each trajectory when the user and reference station have access to each respective orbiter. Although the inclined orbiter does not have significant intervals of access with the users, the orbiter does vary the constellation geometry and therefore diversify measurements.

As shown in Figure 3, there are frequent intervals with no orbiters visible and only a single instance with two orbiters in view simultaneously. This is due to the 15-degree elevation mask imposed on both the user and the reference station.

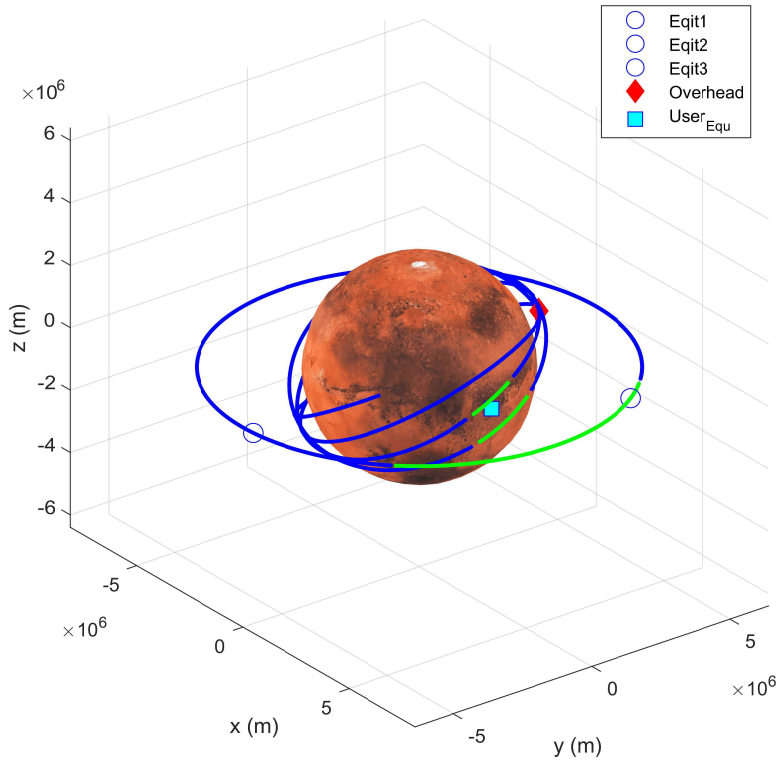

Figure 2. Orbiter trajectories in Mars center Mars fixed (MCMF).

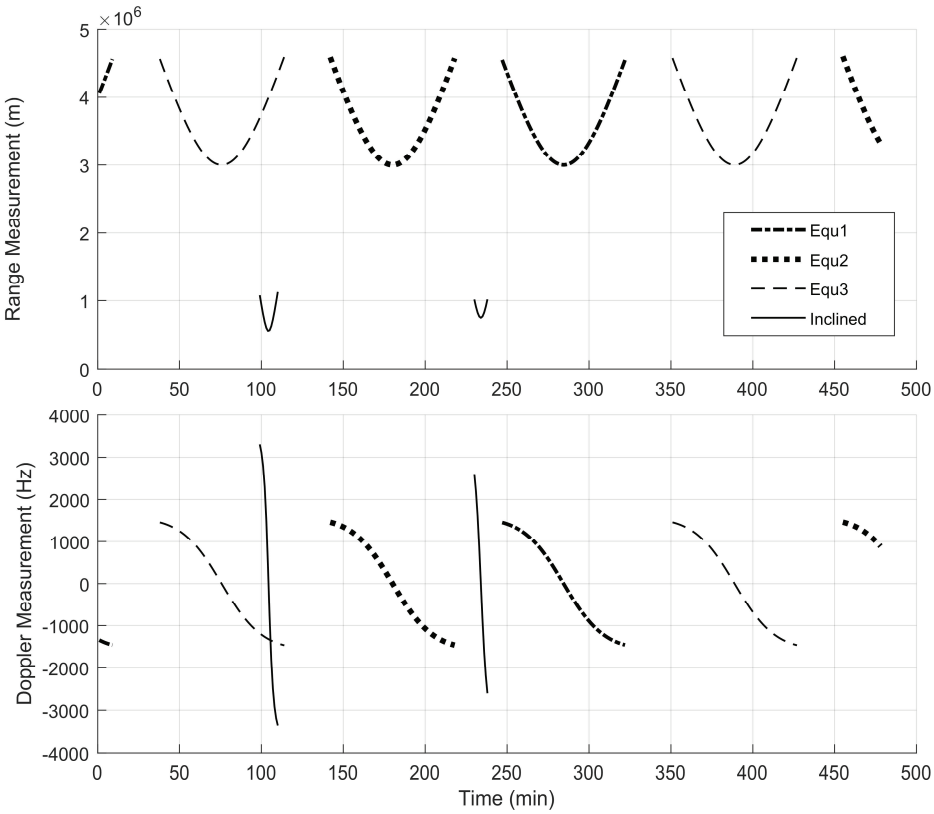

Figure 3. Orbiter measurements.

V. Simulation Setup

Using simulated trajectories of each orbiter propagated in MATLAB, the true Doppler and range measurements of both the user and the reference station were calculated with a sampling rate of one measurement instance per minute. These measurements and the users' knowledge of orbiter ephemeris and velocity were then corrupted with Gaussian error (Table 2). In addition, user clock error was modelled with a stability of 10 E -11 over 60 seconds with orbiter clocks assumed perfect. These error parameters were taken from a similar Mars navigation analysis [9]. A new Gaussian noise value was calculated for each 3D axis at each timestep. All noise was assumed independent, time invariant, and unbiased.

Table 2. 1σ Gaussian error values.

Error Type	Value	Error Type
Satellite Ephemeris Vector (3D)	5 m	Knowledge Error
Satellite Velocity Vector (3D)	1 mm/s	Knowledge Error
Pseudorange Measurement	1 m	Measurement Error
Doppler Measurement	0.5 mm/s	Measurement Error

All simulated orbiters transmitted at the same frequency of 401.5 MHz (UHF) to align with the operating frequencies of current proximity link radios.

The noisy measurement data was sequentially fed into an EKF with the JDR-LOC equations as measurement models. The initial state estimate $\bar{X}_0 = [x_0 \quad y_0 \quad z_0]^T = [R_x \quad R_y \quad R_z]^T$ was the known reference station location. State noise compensation was utilized to prevent rejection of new data and measurement variances were assumed to be known by the filter (through prior empirical data). Once the entire analysis interval was parsed, the EKF was then cleared and rerun with new noisy measurements. This process was repeated 1000 times in a Monte Carlo analysis. No changes were made to the scenario over the Monte Carlo analysis, only the use of a new seed for noise generation.

Because each analysis was the sequential result of an EKF, a modified definition of root mean square error (RMSE) was used to represent the Monte Carlo results. This definition combines the mean and standard deviation of the true positioning error at each timestep of all EKF runs:

$$RMSE_i = \sqrt{\mu_i^2 + \sigma_i^2} \tag{21}$$

Where μ_i is the mean magnitude of 3D positioning error of all 1000 EKF runs at the *i*th timestep and σ_i is the standard deviation of the magnitude of 3D positioning error of all 1000 EKF runs at the *i*th timestep.

VI. Results

The EKF was successfully able to reduce the magnitude of true 3D positioning error to under 15 m in the first 10 minutes for all 1000 runs, and the RMSE to just under 7 m (Figure 4). In addition, the filter was able to maintain an RMSE under 10 m for the entire analysis interval, except for specific instances with large spikes in error. Observing the behavior of the measurements in Figure 3, the spikes in RMSE aligned with the instances where the Doppler measurements approached zero. Although the JDR-LOC expression was modified to remove the divergence of a zero-measured Doppler shift, the effect was still present at a reduced scale. However, the intervals with near zero Doppler shifts can be predicted and therefore their respective measurements can be removed.

Figure 5 shows the results of a repeated Monte Carlo analysis with Doppler shift measurements removed if less than 100 Hz in magnitude. With the removal of near-zero Doppler shift measurements, the RMSE was maintained under 7 meters for the entire analysis interval, with sub-20 m for most of the interval at 3σ.

Error behaviors unique to JDR-LOC were also demonstrated. The bowl shaped dips in RMSE during each orbiters' pass closely aligned with the shape of the range measurements from Figure 3. This is due to the geometry of the JDR-LOC measurement equations. As the satellite orbits increase in altitude, the triangle in Figure 1 becomes significantly taller. This causes the angles θ_u and θ_r to become more sensitive to error, leading to a relationship between the range and overall navigation performance. Another notable behavior was the spike at the 100 minute mark; this was the moment two orbiters were in simultaneous view. Due to the addition of a second set of measurements to the filter, the covariance increased, therefore increasing the reliance on new, noisy measurements.

Ultimately, with this simulation, JDR-LOC was able to achieve positional accuracy of 10 meters within the first 10 minutes and maintain or increase the position accuracy for the remainder of the analysis interval.

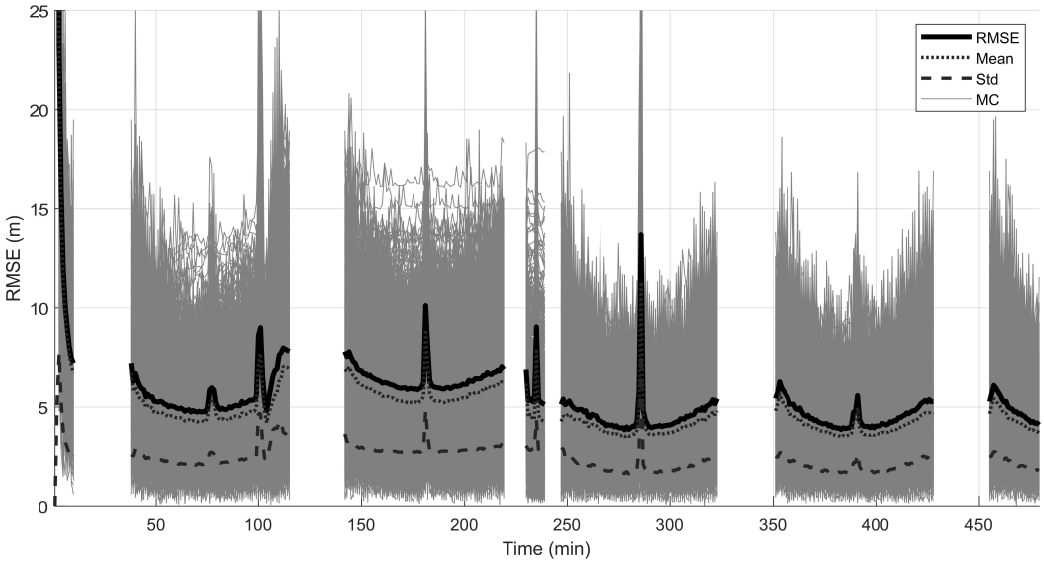

(a) All 1000 EKF Monte Carlo simulations.

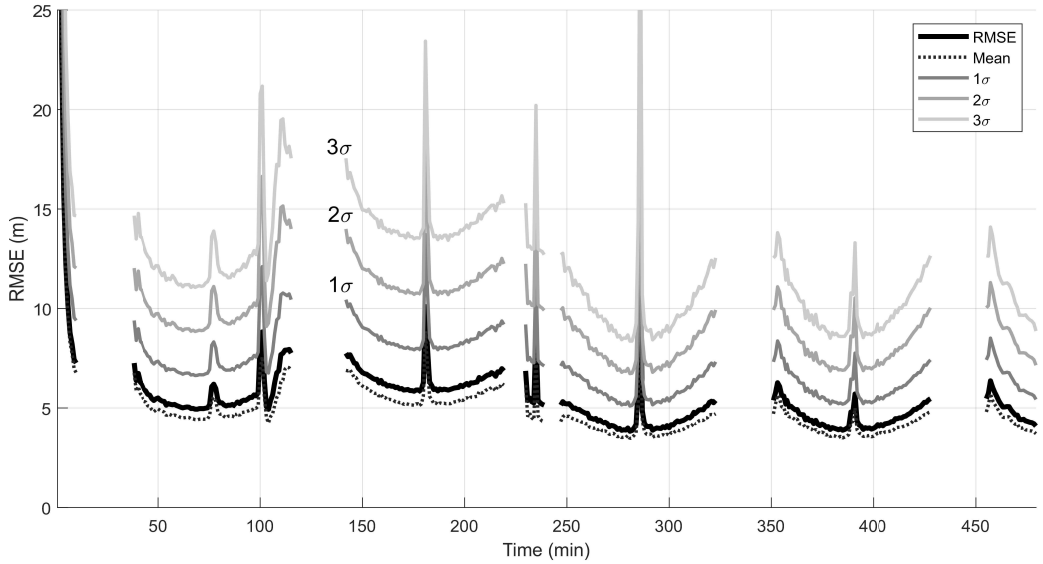

(b) 3σ of EKF sequential error.

Figure 4. RMSE of EKF with Monte Carlo (intervals with no visible orbiters removed).

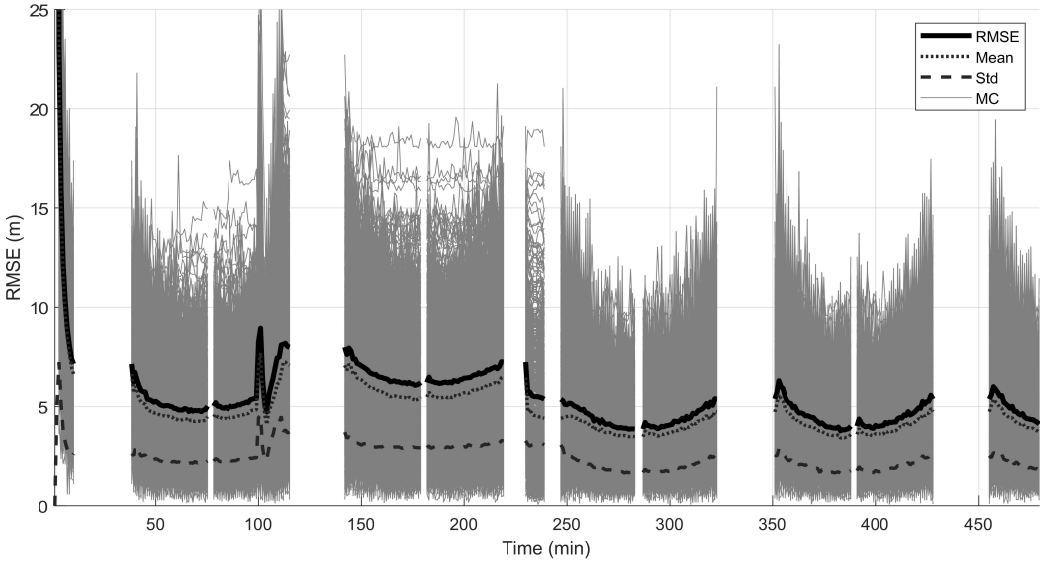

(a) All 1000 EKF Monte Carlo simulations.

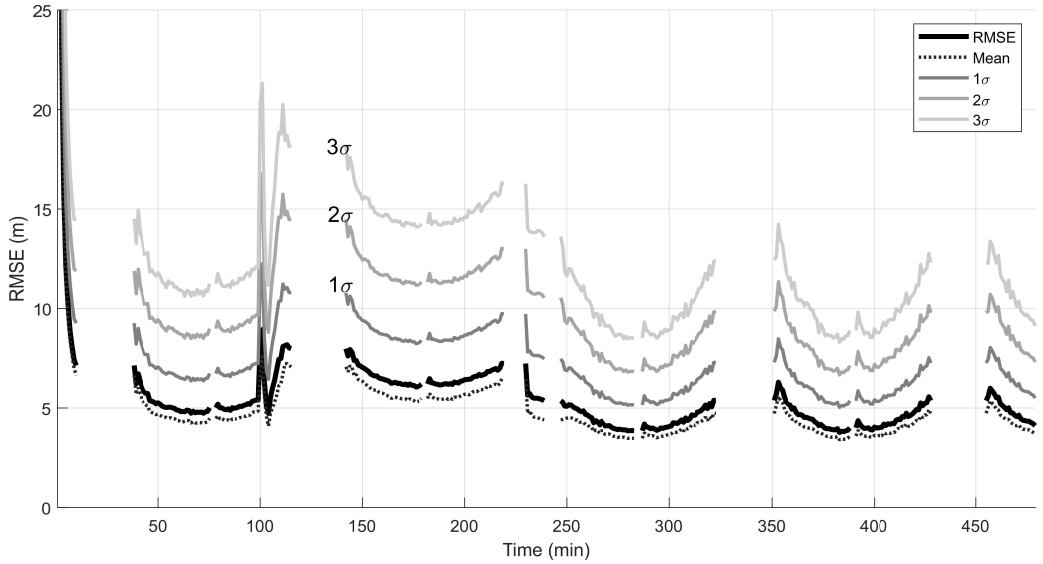

(b) 3σ of EKF sequential error.

Figure 5. RMSE of EKF with Monte Carlo with Doppler shift measurements <100 Hz removed (intervals with no visible orbiters removed).

VII. Sensitivity Analysis

To observe the relationship between each of the embedded Gaussian errors in Table 2 and the overall performance of JDR-LOC, a sensitivity analysis was performed. While keeping all other errors the same, each respective standard deviation was multiplied by an error scaling integer from 1 to 10. For each error parameter and at each error scaling value, the Monte Carlo analysis was reperformed. The sequential RMSE values were averaged (excluding the first 10 minutes) and the resulting mean RMSE value was plotted on Figure 6. For example, while keeping all other error parameters as listed in Table 2, the Doppler measurement 1σ error was multiplied by the error scaling value 2, and the Monte Carlo analysis was rerun with that new set of error standard deviations. The average RMSE of that analysis was plot with respect to the error scaling value 2.

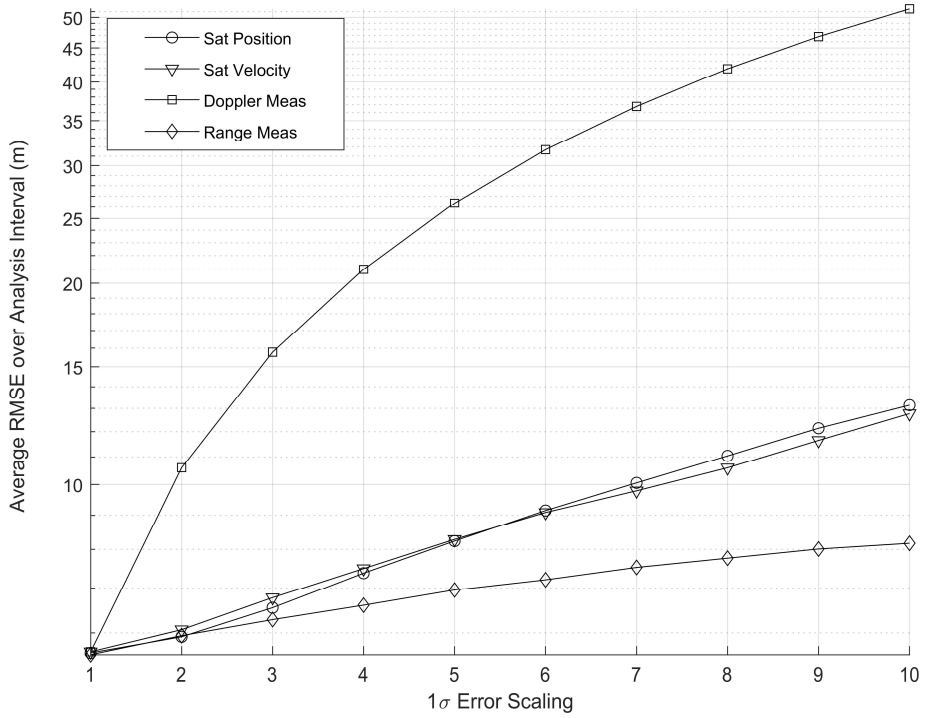

Figure 6. Average RMSE over analysis interval vs. scaled 1σ error.

As expected, JDR-LOC's performance was most sensitive to the Doppler measurement uncertainty. JDR-LOC's robustness to other errors, however, could be seen with the 10-fold increase in orbiter position or velocity error leading to a mean RMSE still under 15 m. Additionally, this method was able to maintain a sub-10 meter RMSE with the same 10-fold increase in range measurement error. An important note to keep in mind is that these results were specific to this scenario. However, the overall behaviors between the error scaling values and JDR-LOC's performance are expected to be similar.

VIII. Conclusion

JDR-LOC enabled accurate and real time positioning on the Martian surface with a minimal navigational architecture. After the first 10 minutes of measurements, JDR-LOC

was able to position a user within 15 m at 3σ. With a maximum of two orbiters in view simultaneously, and only one in view for a significant majority, JDR was able to maintain the RMSE under 10 m and under 20 m at 3σ.

Extrapolating from these results, if only a single equatorial orbiter was available, the user could position themselves to within 10 m in 10 minutes and utilize a sensitive inertial navigation system to provide continuous positioning information until the next orbiter ground pass was available.

Although this analysis was completed on Mars, JDR can be applied to other planets or celestial bodies that do not have existing navigation infrastructures. In a science exploratory mission, an orbiter could be sent with a rover and lander, with the orbiter maintaining a parking orbit while the lander undocks and lands on the surface. Then, the rover could explore the region with the lander acting as a reference station and the orbiter providing measurements. With the components of a single exploratory mission, JDR can enable accurate and autonomous positioning throughout the rover's surface navigation process, therefore decreasing dependence on Earth. Ultimately, JDR can be applied to a myriad of space-based navigation needs that require autonomous positioning with limited resources.

Future work includes introducing estimation of velocity into JDR-LOC. One of the drawbacks JDR-LOC is that any user velocity would impart an unknown bias in the Doppler measurement. Because JDR-LOC is sensitive to Doppler error, this Doppler bias would significantly damage performance. DBAN solved this by utilizing a low drift inertial navigation system to aid in velocity estimation [7]. However, it is possible to estimate the user's velocity through only Doppler measurements. In addition, improved error models will be implemented in the future, including time variance, coupling, and biases. Finally, higher fidelity atmospheric effects will be implemented to observe performance with signal degradation through the atmosphere.

Acknowledgments

The research described in this paper was supported by NASA's Space Communication and Navigation (SCaN) Program. Additional support was provided by a NASA Space Technology Research Fellowship.

References

[1] M. Maurette, "Mars Rover Autonomous Navigation," *Autonomous Robots* 14, 199–208, 2003.

[2] R. Volpe, T. Estlin, S. Laubach, C. Olson, J. Balaram, "Enhanced Mars rover navigation techniques," *Proceedings 2000 ICRA,* Millennium Conference, IEEE International Conference on Robotics and Automation, 2000.

[3] L. Matthies, E. Gat, R. Harrison, B. Wilcox, R. Volpe, T. Litwin, "Mars microrover navigation: Performance evaluation and enhancement," *Autonomous Robots* 2, 291–311, 1995.

[4] E. A. LeMaster, M. Matsuoka, S. M. Rock, "Mars Navigation System Utilizes GPS," *IEEE AESS Systems Magazine,* April 2003.

[5] K.-M. Cheung, W. W. Jun, C. Lee, E. G. Lightsey, "Single-Orbiter Real-Time Relative Positioning for Moon and Mars," International Astronautical Congress (IAC), 2019.

[6] K.-M. Cheung, W. W. Jun, C. Lee, G. Lightsey, "Single-Orbiter Doppler Localization with Law of Cosines (LOC)," IEEE Aerospace Conference, 2019.

[7] W. W. Jun, K.-M. Cheung, J. Milton, C. Lee, G. Lightsey, "Autonomous Navigation for Crewed Lunar Missions with DBAN," IEEE Aerospace Conference, 2020.

[8] D. Simon, Optimal State Estimation Kalman, Hinf, and Nonlinear Approaches Wiley Interscience. Cleveland State University, 2006.

[9] T. A. Ely, R. Anderson, Y. E. Bar-Sever, D. Bell, J. Guinn, M. Jah, P. Kallemeyn, E. Levene, L. Romans, S-C. Wu, "Mars Network Constellation Design Drivers and Strategies," AAS/AIAA Astrodynamics Specialist Conference, 1999.